



Kugeratski, F. G., Batista, M., Lima, C. V. d. P., Neilson, L. J., da Cunha, E. S., de Godoy, L. M., Zanivan, S., Krieger, M. A. and Marchini, F. K. (2018) Mitogen-activated protein kinase kinase 5 regulates proliferation and biosynthetic processes in procyclic forms of *Trypanosoma brucei*. *Journal of Proteome Research*, 17(1), pp. 108-118. (doi:[10.1021/acs.jproteome.7b00415](https://doi.org/10.1021/acs.jproteome.7b00415))

There may be differences between this version and the published version. You are advised to consult the publisher's version if you wish to cite from it.

<http://eprints.gla.ac.uk/151501/>

Deposited on: 08 January 2018

Enlighten – Research publications by members of the University of Glasgow
<http://eprints.gla.ac.uk>

This document is confidential and is proprietary to the American Chemical Society and its authors. Do not copy or disclose without written permission. If you have received this item in error, notify the sender and delete all copies.

The mitogen-activated protein kinase kinase 5 regulates the proliferation and biosynthetic processes in procyclic forms of *Trypanosoma brucei*

Journal:	<i>Journal of Proteome Research</i>
Manuscript ID	pr-2017-00415e.R2
Manuscript Type:	Article
Date Submitted by the Author:	12-Oct-2017
Complete List of Authors:	Kugeratski, Fernanda; Cancer Research UK Beatson Institute, Tumour Microenvironment and Proteomics Laboratory; Carlos Chagas Institute, Fiocruz, Functional Genomics Laboratory Batista, Michel ; Carlos Chagas Institute, Fiocruz, Functional Genomics Laboratory ; Carlos Chagas Institute, Fiocruz, Mass Spectrometry Facility RPT02H Lima, Carla Vanessa; Carlos Chagas Institute, Fiocruz, Functional Genomics Laboratory Neilson, Lisa; Cancer Research UK Beatson Institute, Tumour Microenvironment and Proteomics Lab da Cunha, Elizabeth; Carlos Chagas Institute, Fiocruz, Functional Genomics Laboratory de Godoy, Lyris; Instituto Carlos Chagas, Fiocruz Parana, Zanivan, Sara; Cancer Research UK Beatson Institute, Tumour Microenvironment and Proteomics Lab Krieger, Marco; Instituto Carlos Chagas, Instituto de Biologia Molecular do Parana Marchini, Fabricio; Carlos Chagas Institute, Fiocruz, Functional Genomics Laboratory ; Carlos Chagas Institute, Fiocruz, Mass Spectrometry Facility RPT02H

SCHOLARONE™
Manuscripts

1
2
3 **The mitogen-activated protein kinase kinase 5 regulates the proliferation and**
4 **biosynthetic processes in procyclic forms of *Trypanosoma brucei***
5
6
7

8 Fernanda G. Kugeratski^{1, 2, 3}, Michel Batista^{1, 4}, Carla V. de Paula Lima¹, Lisa J.
9 Neilson², Elizabeth Sousa da Cunha¹, Lyriss M. de Godoy¹, Sara Zanivan^{2, 3}, Marco
10 A. Krieger¹, Fabricio K. Marchini^{1, 4 *}
11
12
13
14

15
16
17 ¹ Carlos Chagas Institute, Fiocruz Parana, Functional Genomics Laboratory, Brazil.
18

19 ² CRUK Beatson Institute, Glasgow, UK.
20

21 ³ University of Glasgow, Glasgow, UK.
22

23 ⁴ Carlos Chagas Institute, Fiocruz Parana, Mass Spectrometry Facility RPT02H,
24 Brazil.
25
26

27
28 * Corresponding author: fabricio.marchini@fiocruz.br
29
30

31 **Abstract**
32

33
34 The pathogenic protozoan *T. brucei* alternates into distinct developmental stages in
35 the mammalian and insect hosts. The mitogen-activated protein kinase (MAPK)
36 signaling pathways transduce extracellular stimuli into a range of cellular responses,
37 which ultimately lead to the adaptation to the external environment. Here, we
38 combined a loss of function approach with stable isotope labelling with amino acids
39 in cell culture (SILAC)-based mass spectrometry (MS) to investigate the role of the
40 mitogen-activated kinase kinase 5 (MKK5) in *T. brucei*. The silencing of MKK5
41 significantly decreased the proliferation of procyclic forms of *T. brucei*. To shed light
42 into the molecular alterations associated with this phenotype, we measured the total
43 proteome and phosphoproteome of cells silenced for MKK5. In the total proteome,
44 we observed a general decrease in proteins related to ribosome and translation as
45
46
47
48
49
50
51
52
53
54
55
56
57
58
59
60

1
2
3 well as down-regulation of several components of the fatty acid biosynthesis
4 pathway. In addition, we observed alterations in the protein levels and
5 phosphorylation of key metabolic enzymes, which point toward a suppression of the
6 oxidative metabolism. Taken together, our findings show that the silencing of MKK5
7 alters cell growth, energy metabolism, protein and fatty acid biosynthesis in procyclic
8 *T. brucei*.
9
10
11
12
13
14
15
16

17 **Keywords**

18
19
20 mitogen-activated protein kinase kinase 5 (MKK5), *T. brucei* , proteomics,
21 phosphoproteomics, energy metabolism, fatty acids biosynthesis.
22
23
24

25 **Introduction**

26
27
28 The Kinetoplastida protozoan *Trypanosoma brucei* is the causative agent of African
29 trypanosomiasis, also known as sleeping sickness. During its complex life cycle, *T.*
30 *brucei* alternates into distinct developmental stages in the mammalian and insect
31 hosts¹. In order to adjust to the different environment, major metabolic and
32 morphological changes are required. In this context, post-translational modifications
33 (e.g. protein phosphorylation) represent a dynamic mechanism that can mediate the
34 prompt adaptation to the conditions encountered in each host, such as temperature,
35 nutrient availability and pH². In fact, in trypanosomatids kinases belonging to the
36 CMGC and STE groups, which comprise the mitogen-activated protein kinase
37 (MAPK) signaling pathways, are overrepresented in comparison to humans³. The
38 MAPK pathway transduce external signals into cellular responses, leading to
39 changes in cell proliferation, survival and morphology, which ultimately
40 accommodate the cellular physiology to the new environment⁴. In these intricate
41 signaling cascades, a MAP kinase kinase kinase kinase (MKKKK, MAPKKKK,
42
43
44
45
46
47
48
49
50
51
52
53
54
55
56
57
58
59
60

1
2
3 MAP4K or STE20) phosphorylates and activates a MAP kinase kinase kinase
4 (MKKK, MAPKKK, MAP3K or STE11), which in turn phosphorylates and activates a
5 MAP kinase kinase (MKK, MAPKK, MAP2K or STE7) that then phosphorylates the
6 conserved threonine and tyrosine residues located in the activation loop of a MAP
7 kinase (MAPK)^{4,5}. In *T. brucei*, the MAPK pathway is composed by 2 MKKKK, 15
8 MKKK, 5 MKK and 15 MAPK³. To date, seven *T. brucei* MAPK have been studied
9 and their involvement in a variety of cellular functions demonstrated. The MAPK
10 KFR1 participates in the response to interferon-gamma in bloodstream forms⁶;
11 MAPK2 is required for the differentiation into procyclic forms⁷; TbECK1 modulates
12 cell growth in procyclic forms⁸; TbMAPK5 controls virulence and differentiation of
13 bloodstream forms⁹; TbMAPK4 confers resistance to temperature stress in procyclic
14 forms¹⁰, TbERK8 is required for cell growth in bloodstream forms¹¹ and MAPK1 is
15 required for proliferation in procyclic forms¹². From the five MKK proteins of *T.*
16 *brucei*, MKK1 and MKK5 have been previously studied. The knockout of these genes
17 in bloodstream forms did not cause changes in cell growth in standard culture
18 conditions; however, defects in proliferation were observed upon exposure to
19 temperature stress¹³. Interestingly, in the same work, western blot analysis
20 suggested that MKK5 expression is higher in the procyclic than in the bloodstream
21 forms of *T. brucei*¹³, which may indicate that the role of this protein is developmental
22 stage-specific. To date, the function of MKK5 in procyclic forms of *T. brucei* has not
23 yet been addressed. The combination of quantitative proteomics and
24 phosphoproteomics with perturbation of kinases and phosphatases is a powerful
25 approach to discover the pathways and substrates regulated by these proteins at a
26 systems level^{12,14-16}. Here, we combined a loss of function approach with SILAC-
27 based proteomics and phosphoproteomics to uncover the role of MKK5 in procyclic
28
29
30
31
32
33
34
35
36
37
38
39
40
41
42
43
44
45
46
47
48
49
50
51
52
53
54
55
56
57
58
59
60

1
2
3 forms of *T. brucei*. Our results revealed that the silencing of MKK5 induces
4
5 significant changes in the proliferation, in the total levels and phosphorylation of
6
7 translation, fatty acid biosynthesis and energy metabolism-related proteins, thus
8
9 indicating that this kinase is involved in the maintenance of homeostasis in procyclic
10
11 forms of *T. brucei*.
12

13 14 15 **Materials and Methods**

16 17 18 **MKK5 RNAi plasmid design, cloning and transfection**

19
20 The DNA sequence of MKK5 (gene ID Tb927.10.5270 or Tb10.70.1800, Uniprot ID
21
22 Q38B76) of *T. brucei brucei* TREU 927 was retrieved from GeneDB database. The
23
24 selection of a specific target region for RNAi and the design of primers were
25
26 performed using the web tool RNAit from TrypanoFAN using the default settings¹⁷.
27
28 The resulting primers, MKK5 forward 5'-AAGTTCACAGGTCAAACCCG-3' and
29
30 MKK5 reverse 5'-GTTTCAGCAACAAGACCA-3', were used to amplify by PCR the
31
32 RNAi target region from the genomic DNA of *T. brucei* Lister 427. The PCR reaction
33
34 was performed using 1 U of Taq DNA polymerase high fidelity (Invitrogen), Platinum
35
36 Taq buffer, 2 mM MgSO₄, 0.4 mM of each primer, 10 mM dNTPs and 100 ng of
37
38 genomic DNA as template. The PCR was performed using one cycle of 94 °C during
39
40 2 minutes, followed by 30 cycles of 94 °C during 30 seconds, 55 °C for 30 seconds
41
42 and 68 °C for 1 minute; a final extension cycle of 68 °C during 5 minutes was
43
44 employed. Prior to cloning, the PCR products were purified using the High pure PCR
45
46 product purification kit (Roche) following the manufacturer's instructions and run in a
47
48 0.8% agarose gel for confirmation of the amplicon size. The PCR product was
49
50 cloned in a modified version of the p2T7-177 plasmid¹⁸, which contained the LacZ
51
52 gene instead GFP. The LacZ cassette of the modified p2T7-177 plasmid was flanked
53
54 by two *XcmI* restriction sites, providing 'T' overhangs after digestion with *XcmI*, which
55
56
57
58
59
60

1
2
3 are then cohesive with the 'A' extremities of the PCR products, thus allowing to use
4 the TA cloning strategy. Moreover, the LacZ gene allows screening the positive
5 colonies by color. For digestion, 2 µg of the plasmid, 10 U of *XcmI* (New England
6 Biolabs), and NEB2 buffer were used, the reaction was incubated at 37 °C for 2h,
7 followed by heat inactivation at 65 °C for 20 minutes. The digestion of the plasmid
8 was confirmed using a 0.8% agarose gel and the corresponding band of the vector
9 was excised and purified from the gel. The vector-insert ligation was performed using
10 1 U of T4 DNA ligase (Invitrogen), ligase buffer, 50 ng of the vector and 1:10 molar
11 ratio vector-insert overnight at 16 °C. The resulting plasmids were transfected by
12 heat shock into DH5α cells. Positive clones were screened by colony PCR and the
13 RNAi target sequence was confirmed by DNA sequencing. From now on, the
14 resulting RNAi MKK5-p2T7177 plasmid to silence MKK5 in *T. brucei* will be referred
15 as MKK5 RNAi plasmid. Prior to transfection, 5 µg of the MKK5 RNAi plasmid was
16 linearized using 8 U of *NotI* HF (New England Biolabs), NEB4 buffer, and BSA at 37
17 °C for 16 hours, followed by heat inactivation at 65 °C for 20 minutes. The linearized
18 MKK5 RNAi plasmid was transfected by electroporation into procyclic forms of *T. brucei*
19 *brucei* Lister 427 clone 29-13¹⁹. For transfection, 4 x 10⁷ cells were washed in
20 electroporation buffer (129 mM NaCl, 1.5 mM KH₂PO₄, 8 mM KCl, 8 mM NaH₂PO₄,
21 1.5 mM MgCl₂, 0.09 mM CaCl₂, 2.4 mM CH₃COONa, pH 7.0), spin at 5,000 x g, 5
22 min at 4 °C and resuspended in 400 µl of the electroporation buffer in a 0.4 cm
23 cuvette (BioRad). Then, 10 µg of linearized plasmid DNA was added to the cuvette
24 and incubated on ice for 10 min. The cuvettes were subject to two pulses of
25 electroporation (1.6 kV, 25 µF, and time constant of 0.8 s) in a Gene Pulse II
26 Electroporation System (BioRad). The resulting transfected cells were cultured in the
27 medium SDM-79 (LGC Biotecnologia)²⁰, supplemented with 10% FBS (Gibco), 15
28
29
30
31
32
33
34
35
36
37
38
39
40
41
42
43
44
45
46
47
48
49
50
51
52
53
54
55
56
57
58
59
60

1
2
3 $\mu\text{g/ml}$ of G418 (Sigma) and 50 $\mu\text{g/ml}$ of hygromycin (Sigma) and incubated at 28 °C
4
5 in 5% of CO₂. The selection was performed using 2.5 $\mu\text{g/ml}$ of phleomycin (Sigma).
6
7 The transcription of the double-stranded RNAi to silence MKK5 is under control of
8
9 two T7 promoters; to trigger the RNAi mechanism 2 $\mu\text{g/ml}$ of tetracycline (Sigma)
10
11 were added in the first day, and 1 $\mu\text{g/ml}$ was added daily in the course of the
12
13 experiments.
14

15 **RT-qPCR**

16
17 To determine MKK5 silencing efficiency we used RT-qPCR. Procytic forms of *T.*
18
19 *brucei* transfected with the MKK5 RNAi plasmid were treated (Tet+) or not (Tet-) with
20
21 tetracycline for 3 and 4 days. The total RNA was isolated from 1×10^8 cells using
22
23 RNeasy Kit (Qiagen) according to manufacturer's instructions. The cDNA synthesis
24
25 was performed using 1 μg of RNA and 1 μM oligo dT, incubated for 10 min at 70 °C.
26
27 Next, 2 μl of Improm-II buffer (Promega), 6 mM MgCl₂, 10 mM dNTPs, 20 U
28
29 RNaseOUT (Life Technologies) and 2 μl Improm-II Reverse
30
31 Transcriptase (Promega) were mixed in a final volume of 20 μl and incubated for 2 h
32
33 at 42 °C. The resulting product was purified using Microcon YM-30 (Millipore) and
34
35 resuspended in water at a concentration of 2 ng/ μl . The primers used to amplify
36
37 MKK5 were designed using PrimerSelect in the DNASTAR software and their
38
39 efficiency was assessed using a standard curve. The primers anneal at the 3'-UTR
40
41 of MKK5 transcript, T_m 60 °C. In each RT-qPCR reaction, 0.5 μM of the forward 5'-
42
43 GGTGTAGAACGACATGTGTATTTATTTAGGTG- 3' and reverse 5'-
44
45 GTCCTCTCACAGTCCTTGCCCG- 3' primers was used, together with 10 ng of
46
47 template and 10 μl of SYBR green (Life Technologies). For normalization, the
48
49 expression levels of Actin, paraflagellar rod protein (PFR) and telomerase reverse
50
51 transcriptase (TERT) were assessed²¹. The reactions were carried out in triplicates
52
53
54
55
56
57
58
59
60

1
2
3 with appropriated non-targeting controls using the Applied Biosystems 7500 Real-
4 Time PCR System. The analysis was performed using the average of the normalized
5 MKK5 mRNA levels for each housekeeping gene and the remaining levels of MKK5
6 in the Tet⁺ cells expressed as a percentage of the MKK5 levels found in the Tet-
7 cells.
8
9

10 11 12 13 **Growth curves**

14
15 To investigate the impact of MKK5 silencing in the cell growth of procyclic forms of *T.*
16 *brucei* we evaluated the growth rate of cells silenced or not for MKK5. For this, two
17 distinct strategies were employed. In the first one, the cell density was assessed
18 every day until cells reached the stationary growth phase using a Neubauer
19 chamber. In the second strategy, cell density was measured every two days using a
20 Z2 Coulter cell counter (Beckman Coulter), followed by a dilution of the original
21 culture to 1 x 10⁶ cells/ml. In the second set-up, the cell growth was assessed for 10
22 days and cells were kept in exponential growth phase.
23
24
25
26
27
28
29
30
31
32

33 34 **MS sample preparation**

35
36 To accurately quantify the global changes induced by MKK5 silencing in *T. brucei* we
37 used a SILAC-based approach^{12,22-24}. The SDM-79 medium without lysine and
38 arginine was prepared in house²⁰. Procyclic forms of *T. brucei* transfected with the
39 MKK5 RNAi plasmid were cultivated in SDM-79 SILAC medium supplemented with
40 10% 10 kDa dialysed FBS (Sigma), 15 µg/ml of G418 (Sigma) and 50 µg/ml of
41 hygromycin (Sigma) either in the presence of 'unlabelled' lysine and arginine (Arg₀
42 and Lys₀) or in the presence of the 'labelled' counterparts (Arg₁₀ and Lys₄). In total,
43 18 mg/l of lysine and 53.75 mg/l of arginine were used. After incorporation of the
44 labelled amino acids (4 days in culture in the SILAC medium), cells were treated with
45 2 µg/ml of tetracycline in the first day of RNAi induction and with 1 µg/ml of
46
47
48
49
50
51
52
53
54
55
56
57
58
59
60

1
2
3 tetracycline in the subsequent three days. Four days post induction, cells were
4
5 harvested and the same number of MKK5 silenced cells (Tet+) was mixed to the
6
7 control cells (Tet-). The experiments were performed in biological triplicates. The
8
9 cells were washed twice with PBS and spin at 8,000 x g for 5 minutes at 4 °C. The
10
11 resulting pellet was lysed in 8M urea buffer containing protease and phosphatase
12
13 inhibitors (Thermo) and the pH was adjusted to 8. For reduction and alkylation, the
14
15 protein mixture was treated with 1 mM DTT (Sigma) for 1h, room temperature;
16
17 followed by 5.5 mM IAA (Sigma) treatment for 45 minutes, room temperature,
18
19 protected from light. Subsequently, sample was diluted 1:6 in 50mM ABC
20
21 (ammonium bicarbonate) and digested overnight with 2.5 µg of Trypsin (Promega).
22
23 In the following day, the tryptic peptides were acidified to pH 2.5 with TFA (Sigma).
24
25 For the analysis of the total proteome, 10 µg of the resulting peptides were desalted
26
27 in C18 stage-tips^{25,26}. For the analysis of the phosphoproteome, TiO₂-based
28
29 phospho-enrichment was performed. The TiO₂ beads (GL Sciences) were
30
31 resuspended in TiO₂ buffer (30 mg/ml DHB, 80% ACN, 0.1% TFA) at a concentration
32
33 of 500 µg/µl. The mixture was incubated for 10 min at 600 rpm. Subsequently, the
34
35 beads were added to the peptides at a 5:1 ratio and incubated during 1h in rotor
36
37 wheel at room temperature. Then, the mixture was spin at 3,000 rpm and the
38
39 supernatant was collected and subjected to two additional rounds of incubation with
40
41 TiO₂ beads. The phosphopeptides bound to the TiO₂ beads were resuspended in
42
43 washing buffer I (30% ACN, 3% TFA), placed in a C8 stage-tip and spin at 2,600 rpm
44
45 for 2 minutes. The wash with washing buffer I was repeated. Subsequently, three
46
47 washes with washing buffer II (80% ACN, 0.3% TFA) were performed. Three
48
49 sequential elution with 15% ammonium hydroxide in 40% ACN were performed.
50
51
52
53
54
55
56
57
58
59
60

1
2
3 Samples were speed vacuum dried to eliminate the ACN and resuspended in buffer
4 A (0.5% acetic acid). Then, phosphopeptides were purified in C18 stage-tips^{25,26}.
5
6

7 **MS data acquisition**

8
9 The peptides were loaded onto an EASY-nLC system (Thermo Fisher Scientific)
10 coupled online to the mass spectrometer Q-Exactive HF (Thermo Fisher Scientific).
11
12 The chromatography was carried out in a 20 cm fused silica emitter, 75 μm inner
13 diameter (New Objective) packed in house with Reprosil Pur Basic 1.9 μm (Dr.
14 Maisch GmbH). For peptide elution, buffer A (0.1% formic acid) and Buffer B (80%
15 ACN, 0.1% formic acid) were used. For the total proteome, a 250 min gradient of 300
16 nl/min with 2% to 30% buffer B was used. For each fraction of the phosphoproteome,
17 a 120 min gradient of 300 nl/min with 2% to 42% buffer B was used. The eluting
18 peptides were ionized and injected into the mass spectrometer via electrospray,
19 spray voltage 2.1 kV, capillary heater 200 °C. The mass range for the full MS scan
20 was 375-1,500 m/z with a resolution of 60,000 at 250 Th. From total proteome and
21 phosphoproteome fractions, the top 15 and top 10 most intense ions, respectively,
22 were isolated for higher-energy collision dissociation (HCD) fragmentation. The mass
23 window for precursor ion selection was 1.4 m/z. The threshold for triggering MS2
24 was 1.8E5 for the total proteome and 1.0E4 for the phosphoproteome. The relative
25 collision energy used was 27 and the mass resolution for the MS2 was 15,000. The
26 singly charged ions were excluded and the ions that have been isolated for MS/MS
27 were added to an exclusion list for 30 sec (total proteome) and 20 sec
28 (phosphoproteome fractions). MS data were acquired using the Xcalibur software
29 (Thermo Fisher Scientific) and raw data was processed using the MaxQuant
30 computational platform.
31
32
33
34
35
36
37
38
39
40
41
42
43
44
45
46
47
48
49
50
51
52
53
54

55 **MS data processing and analysis**

1
2
3 MaxQuant software version 1.5.0.36 coupled to the Andromeda search engine^{27,28}
4
5 were used to process the raw data with the following settings: Multiplicity 2 (labels
6
7 Arg₁₀ and Lys₄); variable modifications Acetyl (Protein N-term), Oxidation (M) and
8
9 Phospho (STY); fixed modification Carbamidomethyl (C); digestion mode Trypsin,
10
11 maximum 2 missed cleavages. The re-quantify parameter was enabled. The curated
12
13 reference proteome used for peptide identification was downloaded from
14
15 Uniprot *Trypanosoma brucei* TREU 927 (8,587 entries). For identification, the false
16
17 discovery rates (FDRs) at the protein and peptide level were set to 1%. For
18
19 quantification, only unique peptides with minimum 2 ratio counts were used. The
20
21 analysis of the data was done using Perseus version 1.5.2.11²⁹. Reverse peptides,
22
23 potential contaminants and only identified by modification site (for the proteome)
24
25 were removed. Only the class 1 phosphosites, as determined by localization
26
27 probability ≥ 0.75 and score difference > 5 , were considered for the analysis. The
28
29 normalized SILAC ratios from the MaxQuant tables of each biological replicate were
30
31 \log_2 transformed and the intensities \log_{10} . For downstream analyses, we required
32
33 that proteins and phosphosites were quantified in at least two out of three biological
34
35 replicates. The up-regulated and down-regulated proteins were defined based on the
36
37 Significance B statistical test (Benjamini-Hochberg FDR 5%)²⁷, which was calculated
38
39 for each replicate separately. We considered as regulated proteins and
40
41 phosphorylation sites significantly regulated in at least two out of three individual
42
43 biological replicates and with standard deviation lower than the averaged SILAC
44
45 ratio. To determine the Gene Ontology (GO) categories enriched among the subset
46
47 of up-regulated and down-regulated proteins we used Fisher's test (Benjamini-
48
49 Hochberg FDR 5%). For the protein-protein interaction analysis, we used the Uniprot
50
51 IDs of the regulated proteins and phosphorylation sites for the search in STRING,
52
53
54
55
56
57
58
59
60

1
2
3 version 10.0, using the default settings³⁰. The output files were uploaded in
4
5 Cytoscape Version 3.4.0 for visualization of the networks. The mass spectrometry
6
7 proteomics and phosphoproteomics data have been deposited to the
8
9 ProteomeXchange Consortium via the PRIDE partner repository with the dataset
10
11 identifier PXD007910.
12

13 14 15 16 **Results**

17 18 19 **The silencing of MKK5 is detrimental to the proliferation of procyclic forms of** 20 21 ***T. brucei*** 22

23
24 To investigate the role of MKK5 in procyclic forms of *T. brucei* we have used a stable
25
26 inducible RNAi-based loss of function approach. For this, we selected a target region
27
28 unique for MKK5 using the web tool RNAi¹⁷. This fragment was amplified by PCR
29
30 and cloned into a modified version of the vector p2T7-177¹⁸. Procyclic forms of *T.*
31
32 *brucei* were transfected by electroporation with the MKK5 RNAi plasmid. After
33
34 selection, the MKK5 silencing was induced via addition of tetracycline in the cultures
35
36 and cells were used for functional experiments (Figure 1 A).
37
38

39
40 To assess the silencing efficiency, we isolated the mRNA from cells treated or not
41
42 with tetracycline for three and four days and the levels of remaining MKK5 transcripts
43
44 were determined by RT-qPCR. At day three, the remaining levels of MKK5 were
45
46 approximately half than those observed in control cells, whereas at day four, only
47
48 25% of MKK5 mRNA was still present in comparison to the control cells (Figure 1 B).
49
50 Subsequently, to investigate the role of MKK5 in the proliferation of procyclic forms
51
52 of *T. brucei*, we evaluated the growth rate of parasites silenced or not for MKK5
53
54 growing in SDM-79 supplemented with dialyzed serum using two different
55
56 approaches. In the first one, we continuously measured the number of cells in a time
57
58
59
60

1
2
3 course until the parasites reached the stationary phase of growth. In the second set-
4
5 up, parasites were maintained in exponential phase of growth and the cell density
6
7 was measured every second day from day 2 to day 10 post-induction, which allowed
8
9 to assess the effects of MKK5 silencing for longer. In both experimental conditions
10
11 the silencing of MKK5 significantly decreased the growth rate of procyclic *T. brucei*
12
13 (Figures 1C and 1D). We next investigated the growth of procyclic cells in SDM-79
14
15 supplemented with regular FBS, and also in this condition we observed a significant
16
17 decrease in the growth rate (Figure 1E). To shed light into the molecular alterations
18
19 underpinning the defects in cell proliferation upon MKK5 silencing we employed an
20
21 unbiased SILAC-based MS approach. This workflow allows an accurate
22
23 quantification of the proteins and phosphorylation sites modulated upon MKK5
24
25 knockdown (Figure 2).
26
27
28
29

30 **SILAC medium**

31
32 To replace the unlabeled lysine and arginine amino acids by the heavy isotope-
33
34 labelled counterparts, we have prepared in house the SDM-79 medium without these
35
36 amino acids. To determine whether the medium prepared in house was suitable for
37
38 *T. brucei* culture, we compared the growth of *T. brucei* in our medium with the
39
40 commercially available one from LGC. Our results show that the ability of *T. brucei* to
41
42 grow in both commercial and in house prepared SDM-79 culture medium was
43
44 indistinguishable (Supplementary figure 1A). Subsequently, to decrease the costs
45
46 related to the labelled amino acids, we conduct growth tests using 50%, 25%, 12.5%
47
48 of the original concentration of lysine and arginine. We observed that when we used
49
50 50% or 25% of the original concentration of lysine or arginine present in the
51
52 conventional SDM-79 medium there was no significant differences in the growth of
53
54 the parasites. We only observed proliferation defects when the concentration was
55
56
57
58
59
60

1
2
3 decreased to 12.5% or when lysine and arginine were completely removed
4
5 (Supplementary figures 1B and 1C). Likewise, when using 25% of both lysine and
6
7 arginine the proliferation of *T. brucei* was comparable to the counterpart cells
8
9 growing in the medium containing the full amount of these amino acids
10
11 (Supplementary figure 1D). Additionally, we tested the incorporation rate of labelled
12
13 amino acids using 100%, 50% and 25% or the original concentration of lysine and
14
15 arginine and we observed that the rate of labelled amino acids incorporation was
16
17 efficient in the three conditions: more than 98% of the peptides were labelled after 4
18
19 days growing in the SILAC medium.
20
21

22
23 **Global proteomics and phosphoproteomics analysis of MKK5 knockdown cells**
24
25 **reveals alterations in translation, fatty acid biosynthesis and energy**
26
27 **metabolism-related proteins and phosphorylation sites**
28
29

30
31 In the SILAC-based total proteome of *T. brucei* silenced for MKK5, we
32
33 unambiguously identified 3,965 proteins and accurately quantified 3,024 proteins in
34
35 at least 2 out of 3 biological replicates (Supplementary Table 1). To determine in an
36
37 unbiased manner alterations in the abundance of proteins belonging to specific gene
38
39 ontology categories we used the 1D enrichment analysis³¹, and found that the
40
41 abundance of proteins related to ribosome and translation was significantly reduced
42
43 upon MKK5 silencing. These include the GOMF structural constituent of ribosome
44
45 (p-value 6.73E-26), GOCC ribonucleoprotein complex (p-value 1.72E-24), GOBP
46
47 translation (p-value 4.85E-24) and GOCC ribosome (p-value 8.29E-24) (Figure 3).
48
49

50
51 Subsequently, to ascertain the significantly up-regulated and down-regulated
52
53 proteins upon MKK5 silencing we used the significance B test in each replicate
54
55 separately (Benjamini-Hochberg FDR 0.05). In the supplementary table 1, we have
56
57 indicated the regulated proteins and reported the FDRs for each individual replicate.
58
59
60

1
2
3 To determine the reproducibly regulated proteins, we required that the regulation
4 occurred in at least two out of the three biological replicates and that the standard
5 deviation was lower than the averaged SILAC ratio. Using this cut-off we found 11
6 proteins significantly up-regulated and 27 proteins down-regulated (Figure 4A and
7 Table 1).
8
9

10
11
12 To determine the gene ontology (GO) categories and KEGG pathways
13 overrepresented in the subset of regulated proteins, we conducted an enrichment
14 analysis. Among the up-regulated proteins, the KEGG pathway TCA cycle was
15 enriched (Figure 4B). In the subset of down-regulated proteins, GO categories and
16 KEGG pathways related to fatty acid biosynthesis, endoplasmic reticulum (ER),
17 carboxylic acid metabolic process and transferase activity were enriched, thus
18 indicating these functions were reduced in procyclic cells silenced for MKK5 (Figure
19 4C).
20
21
22
23
24
25
26
27
28
29
30
31

32
33 Next, to determine the changes induced by the silencing of MKK5 in the
34 phosphoproteome of *T. brucei* and therefore to gain insights regarding the potential
35 targets of this kinase, we used a sequential TiO₂-based enrichment coupled to
36 SILAC-based MS. Using 250 µg of starting material and three sequential TiO₂
37 incubations, we identified 1,482 class 1 phosphosites: 1,267 on serine residues
38 (85.5%), 208 on threonine (14.0%) and 7 on tyrosine (0.05%). The 914 phosphosites
39 quantified in at least 2 out of 3 biological replicates were used for downstream
40 analyses (Supplementary table 2). We normalized the levels of the phosphorylation
41 sites to the total levels of the corresponding protein when it was quantified in the total
42 proteome. For those sites where the total levels of the corresponding protein were
43 not quantified we maintained the SILAC ratio value for the phosphorylation site. In
44 total, 88.7% of the phosphorylation sites could be normalized and are indicated in
45
46
47
48
49
50
51
52
53
54
55
56
57
58
59
60

1
2
3 the Supplementary table 2. Then, to determine the significantly and reproducibly
4 regulated phosphorylation sites we used the same criteria previously described for
5 the total proteome. This analysis resulted in 24 phosphorylation sites significantly up-
6 regulated and 8 significantly down-regulated (Table 2). The most up-regulated and
7 down-regulated phosphorylation sites, respectively, were on the serine 284 of the
8 alpha subunit of pyruvate dehydrogenase E1 (PDHE1 α) and on the serine 207 of the
9 delta subunit of the eukaryotic translation initiation factor 2B (eIF2B δ)
10 Supplementary figure 2). Interestingly, these residues are conserved with the
11 corresponding human proteins (Supplementary figures 3 and 4). Moreover, proteins
12 that can influence rearrangements of the cytoskeleton, intracellular trafficking and
13 cell migration were differentially phosphorylated. This was the case for the up-
14 regulated phosphorylation sites on serine 95 of beta tubulin (Q4GYY6), threonine
15 757 of intraflagellar transport protein IFT88 (Q386Y0), serine 2,053 of the
16 microtubule-associated protein (Q389U9) and the down-regulated site on the serine
17 469 of kinesin-like protein (Q38CW6). Additionally, ubiquitin-related proteins had
18 phosphorylation levels increased upon MKK5 silencing, these sites were on the
19 serine 2 of ubiquitin-fold modifier 1 (Q57UL0), serine 9 of ubiquitin carboxyl-terminal
20 hydrolase (Q385P1) and serine 184 of ubiquitin carboxyl-terminal hydrolase
21 (Q583R5).

22
23
24
25
26
27
28
29
30
31
32
33
34
35
36
37
38
39
40
41
42
43
44
45
46 Finally, in order to integrate the proteomic and phosphoproteomic data and to gain
47 insights regarding the functional relationship among the regulated proteins and
48 phosphorylation sites we used STRING. In the network generated from this analysis,
49 we can observe that several mitochondrial proteins involved in energy metabolism
50 were linked. Additionally, components of the fatty acid biosynthesis pathway and
51 cytoskeleton/cell motility-related proteins were connected (Figure 5).
52
53
54
55
56
57
58
59
60

Discussion

Here, we show for the first time the involvement of the protein MKK5 in cell growth, energy metabolism, translation and fatty acid biosynthesis in procyclic forms of *T. brucei*.

Using different conditions to assess *T. brucei* the cell growth we found that the silencing of MKK5 significantly decreased the proliferation of procyclic cells. The effects on cell growth observed in our study were more pronounced when the SDM-79 medium was supplemented with dialyzed FBS, with more than 30% decrease in cell number in comparison to 15% decrease in the presence of regular FBS. This finding may suggest that either low molecular weight soluble factors or free amino acids found in the regular FBS can function as upstream regulators of this pathway. This observation is particularly relevant considering that procyclic *T. brucei* exist in the insect midgut, an environment deprived of glucose, where the energetic needs are met via amino acids catabolism. In the literature, the knockout of MKK5 in bloodstream forms did not alter the cell growth¹³, thus indicating that the requirement for this kinase is likely developmental stage-specific.

The global SILAC-based approach employed in our study provided valuable insights regarding the role of MKK5. First, using the 1D analysis, we observed a general decrease in proteins related to ribosome and translation. Interestingly, the most down-regulated phosphorylation site quantified in our study was on the delta subunit of the eukaryotic translation initiation factor 2B (eIF2B δ), which is part of the regulatory subcomplex of the holoenzyme. eIF2B is a multi-subunit protein critical for the regulation of the initiation of protein synthesis and its activity is inhibited in response to different types of stress^{32,33}. The precise role of the phosphorylation site

1
2
3 we found regulated on the activity of eIF2B complex is still unknown. One hypothesis
4 is that the modulation of this site may regulate protein synthesis initiation and be
5
6 linked to the general decrease in the abundance of proteins related to translation
7
8 observed upon MKK5 silencing. As a future step to characterize this further,
9
10 mutagenesis of this residue coupled to protein synthesis profiling strategies could be
11
12 employed.
13
14

15
16 Another interesting finding of our study corresponds to the down-regulation of
17
18 several components of the fatty acid biosynthesis pathway. *T. brucei* exploits the
19
20 endoplasmic reticulum (ER)-based elongase (ELO) pathway for fatty acid
21
22 biosynthesis³⁴. In this pathway, the enzymes elongases (ELO1-3), which are integral
23
24 membrane proteins residents in the ER, extend the fatty acid chains: ELO1 extends
25
26 C4 to C10, ELO2 extends C10 to C14, and ELO3 extends C14 to C18³⁵. Here, we
27
28 found that the knockdown of MKK5 in *T. brucei* decreased the protein levels of the 2
29
30 elongases (Q57UP8, Q57UP6); 2 desaturases (Q587G0 and Q57YK1), and of the
31
32 fatty acyl CoA synthetase 2 (Q38FB9). In addition, two other enzymes that provide
33
34 acetyl-CoA for lipid biosynthesis were down-regulated upon MKK5 silencing:
35
36 carnitine O-acetyltransferase (Q386T6) and acetyl-coenzyme A synthetase
37
38 (Q57XD7)³⁶. Because MKK5 silencing alters the protein levels of different
39
40 components of the fatty acid biosynthesis pathway, this kinase could ultimately
41
42 impact key cellular functions, such as energy storage, composition and fluidity of the
43
44 plasma membrane.
45
46
47
48

49
50 In addition, the silencing of MKK5 altered the total levels and phosphorylation of
51
52 proteins involved in energy metabolism. While bloodstream forms of *T. brucei*
53
54 produce ATP via glycolysis, the procyclic forms are more flexible; they are able to
55
56 adapt to distinct carbon sources and to produce energy using both the glycolytic and
57
58
59
60

1
2
3 oxidative pathways^{37,38}. In the subset of up-regulated proteins, the KEGG pathway
4 tricarboxylic acid (TCA) cycle was enriched and metabolic enzymes of the TCA cycle
5 were linked in the STRING-based network. The enzyme citrate synthase (Q388Q5)
6 that catalyzes the conversion of acetyl-CoA and oxaloacetate into citrate, the first
7 reaction of the TCA cycle; and the enzyme isocitrate dehydrogenase (Q387G0), that
8 catalyzes the oxidative decarboxylation of isocitrate, producing alpha-ketoglutarate,
9 CO₂ and NADH, were up-regulated. Of note, procyclic *T. brucei* can use parts of the
10 TCA cycle for different purposes, such as for the degradation of proline and
11 glutamate into succinate, generation of malate for gluconeogenesis and transport of
12 acetyl-CoA from the mitochondria to the cytosol for fatty acids biosynthesis³⁹. In fact,
13 it has been proposed that the acetyl-CoA produced in the mitochondria can be
14 exchanged to the cytoplasm via citrate and then used for lipid synthesis⁴⁰. Moreover,
15 we observed an up-regulation of Succinyl-CoA:3-ketoacid-coenzyme A transferase
16 (ASCT), which converts acetyl-CoA into acetate. In this pathway, the acetate
17 production occurs in two steps: first, ASCT transfers the CoA of acetyl-CoA to
18 succinate, generating acetate and succinyl-CoA, which is then converted into
19 succinate by the enzyme succinyl-CoA synthetase⁴¹. Noteworthy, the ASCT pathway
20 also produces ATP and together with the TCA cycle and the respiratory chain
21 comprise the three mitochondrial pathways generating ATP in the insect-stage *T.*
22 *brucei*^{37,38}. Intriguingly, the most up-regulated phosphorylation site detected in
23 response to MKK5 silencing was on the alpha subunit of pyruvate dehydrogenase
24 E1 (PDHE1 α), which catalyzes a rate-limiting step in the conversion of pyruvate into
25 acetyl-CoA. PDHE1 α is part of the pyruvate dehydrogenase complex that links
26 glycolysis to the TCA cycle. In procyclic cells, a decreased growth rate was observed
27 in cells silenced for PDHE1 α ³⁷. In humans, the enzymatic activity of the pyruvate
28
29
30
31
32
33
34
35
36
37
38
39
40
41
42
43
44
45
46
47
48
49
50
51
52
53
54
55
56
57
58
59
60

1
2
3 dehydrogenase complex is inhibited via phosphorylation of any of the three sites of
4
5 PDHE1 α : serine 232, serine 293, and serine 300⁴². Using multiple sequence
6
7 alignment, we found that the up-regulated phosphorylation site at serine 284 of *T.*
8
9 *brucei* PDHE1 α aligns with the serine 293 of the human PDHE1 α , and out of the
10
11 three regulatory sites of the human enzyme, this is the only one conserved with the
12
13 *T. brucei* protein. In fact, a previous report that compared the sequence of the
14
15 human PDHE1 α with representative species from other taxonomic groups, reported
16
17 one phosphosite for *T. brucei*⁴³. If this phosphorylation site has also an inhibitory
18
19 function in the pyruvate dehydrogenase complex of *T. brucei* as it does in the
20
21 human, we can anticipate a decreased production of acetyl-CoA from pyruvate,
22
23 which in turn could impact both ATP production and lipid biosynthesis. Additionally,
24
25 among the down-regulated proteins we found succinate dehydrogenase (Q38EW9),
26
27 an enzyme of the Complex II of the respiratory chain; and, an electron transfer
28
29 protein (Q57YX5). The down-regulation of components of the respiratory chain could
30
31 indicate an overall decrease in the production of ATP using this route. Overall, our
32
33 data suggests that MKK5 silencing affects the metabolic homeostasis of the insect-
34
35 stage *T. brucei* by regulating the total levels and phosphorylation of several
36
37 metabolic enzymes. As a future step to unravel the consequences of MKK5 silencing
38
39 in the overall energy production, metabolomics and tracing studies could prove
40
41 informative.
42
43
44
45
46
47

48 The changes in phosphorylation measured in our study are likely an indirect effect of
49
50 MKK5 knockdown, since we did not detect regulated phosphorylation sites within the
51
52 activation loop of MAP kinases, which are the canonical targets of MKK proteins. We
53
54 found the threonine and tyrosine residues located in the activation loop of one MAPK
55
56 (Q381A7) phosphorylated in this study; however, these sites were not regulated
57
58
59
60

1
2
3 upon MKK5 silencing. The fact we did not identify multiple MAPK phosphorylated
4
5 may reflect the amount of starting material used in our study, which was 250 μ g.
6
7 Previous phosphoproteomic studies performed in *T. brucei* that used from 2.5-10 mg
8
9 of starting material have identified from 4 to 9 MAPKs phosphorylated^{12,24,44}. To date,
10
11 in trypanosomatids, two MKK-MAPK pairs have been identified. The orthologue of *T.*
12
13 *brucei* MKK5 in *Leishmania mexicana* has been shown to phosphorylate the MAPK
14
15 LmxMPK4 *in vitro*⁴⁵. Moreover, in *L. major*, MKK1 has been shown to phosphorylate
16
17 MPK3 and these kinases regulate the flagellar length⁴⁶. To unravel the relationship
18
19 among the components of the MAPK pathway in *T. brucei*, different protein-protein
20
21 interaction (PPI)-based approaches could prove informative, such as yeast two-
22
23 hybrid, co-localization assays or pull-down analyses.
24
25
26
27
28
29
30

31 **Conclusion**

32
33
34 We have shown for the first time that MKK5 influences the proliferation of procyclic
35
36 forms of *T. brucei*. Furthermore, we have quantified the molecular alterations at the
37
38 protein and phosphorylation levels upon MKK5 silencing using a SILAC-based MS
39
40 approach. Our work provides a global overview of MKK5-responsive pathways and
41
42 phosphorylation sites, which can be used as a valuable resource to further explore
43
44 the role of this protein. Our findings indicate that MKK5 regulates cell growth, protein
45
46 translation, fatty acids biosynthesis and energy metabolism-related proteins and
47
48 phosphosites. Collectively, these findings can open new avenues to be explored in
49
50 future work to dissect the mechanistic role of this kinase.
51
52
53
54
55

56 **Supporting information**

57
58
59
60

1
2
3 **Supplementary figure 1:** Comparison of the growth of procyclic *T. brucei* in the
4 commercial SDM-79 from LGC with the SDM-79 produced in house and evaluation
5 of cell growth using decreasing concentration of lysine (K) and arginine (R).
6
7

8
9
10 **Supplementary figure 2:** Annotated spectra of the most regulated phosphorylation
11 sites on eIF2B δ and PDHE1 α .
12
13

14
15 **Supplementary figure 3:** The phosphorylation site on serine 207 of *T. brucei* eIF2B
16 δ (Q4FKA6) aligns with the serine 181 of human eIF2B δ (Q9UI10).
17
18

19
20 **Supplementary figure 4:** The phosphorylation site on serine 284 of *T. brucei*
21 PDHE1 α (Q388X3) aligns with the serine 293 of human PDHE1 α (P08559).
22
23

24
25 **Supplementary table 1:** Total proteome of *T. brucei* silenced for MKK5. Table
26 report the list of quantified proteins with their corresponding IDs, SILAC ratios, and
27 FDR values.
28
29

30
31 **Supplementary table 2:** Phosphoproteome of *T. brucei* silenced for MKK5. Table
32 report the list of quantified phosphorylation sites with their corresponding IDs, SILAC
33 ratios, and FDR values.
34
35
36
37
38
39
40
41
42
43

44 **Acknowledgements**

45
46 We are grateful to Dr. David Horn for kindly providing the p2T7^{TAblue} plasmid, to
47 Oswaldo Cruz Foundation (FIOCRUZ) and National Council of Technological and
48 Scientific Development (CNPq) for funding.
49
50
51

52 **Conflict of interest**

53
54
55 The authors declare no conflict of interest.
56
57
58
59
60

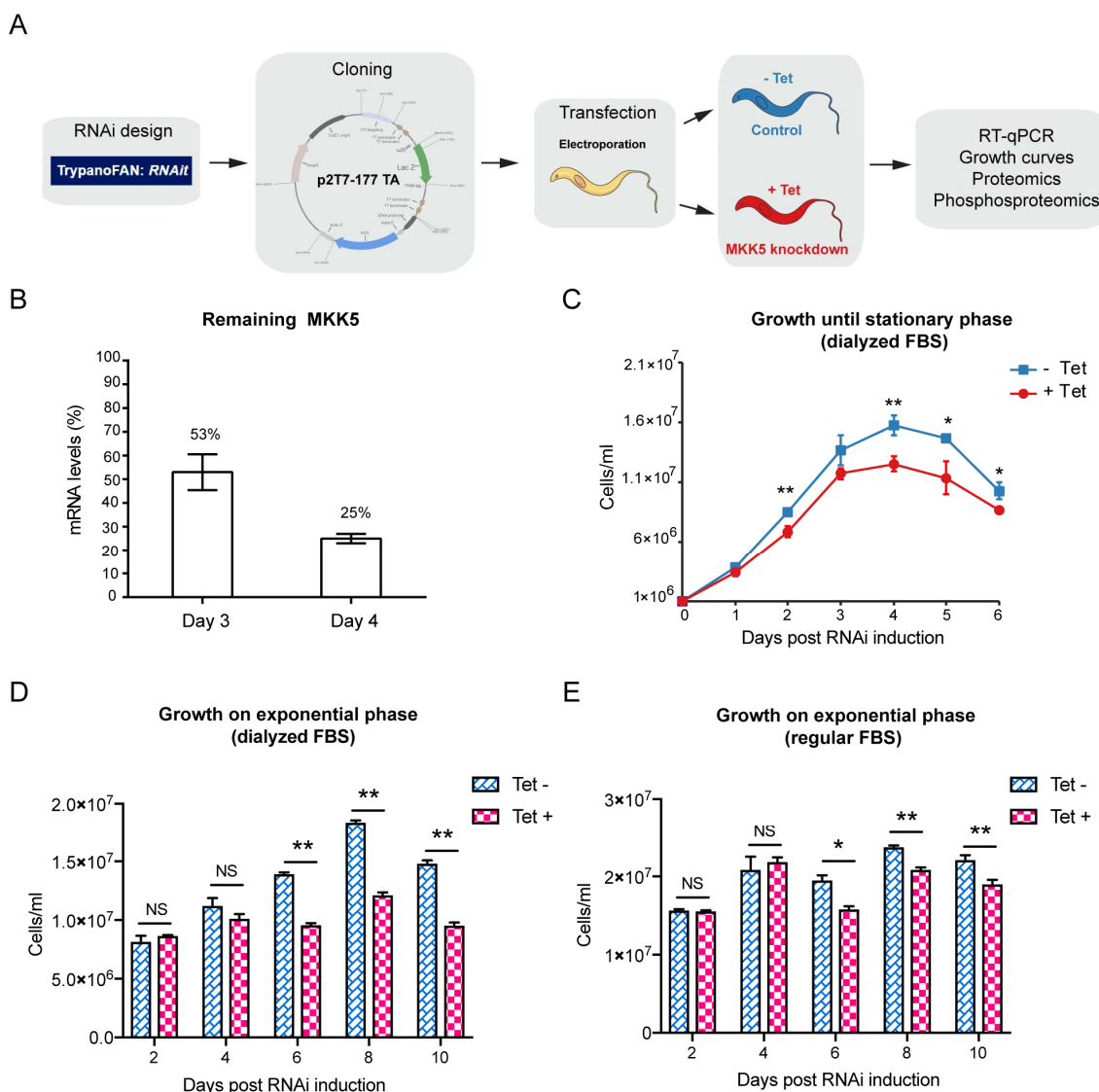


Figure 1: The silencing of MKK5 is detrimental for the growth of procyclic forms of *T. brucei*. (A) Experimental workflow used for RNAi construct design, cloning and transfection. Trypanosoma image adapted from medical servier art. (B) MKK5 silencing efficiency determined by RT-qPCR. The results are expressed as a percentage in comparison to control cells. mRNA levels were normalized to Actin, PFR and TERT. (C) Growth curve until stationary phase in dialyzed FBS. (D) Long-term growth curve in dialyzed FBS. (E) Long-term growth curve in regular FBS.

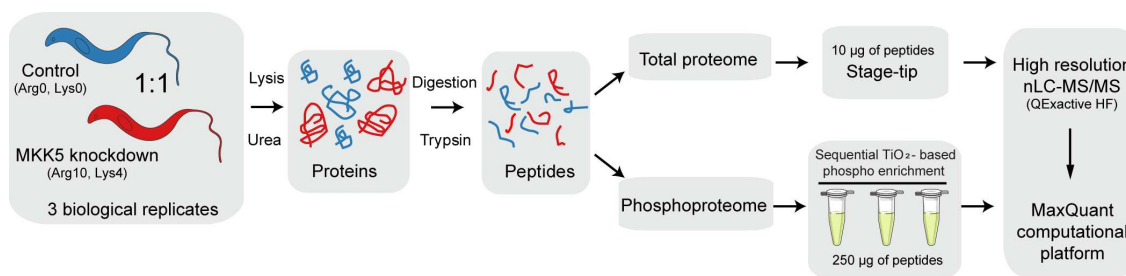


Figure 2: SILAC-based MS proteomics and phosphoproteomics workflow. *T. brucei* were SILAC labelled and the knockdown of MKK5 was induced via addition of tetracycline into the cultures for four days. Then, the same number of induced and non-induced cells was mixed, cells were lysed and proteins digested into peptides. For the analysis of the total proteome, peptides were purified in stage-tips and then run in the mass spectrometer. For the analysis of the phosphoproteome, the phosphopeptides were enriched using three sequential incubations with TiO₂ and then run in the mass spectrometer QExactive HF. All experiments were performed in biological triplicates and the raw data was processed and analyzed using the MaxQuant computational platform. Trypanosoma image adapted from medical servier art.

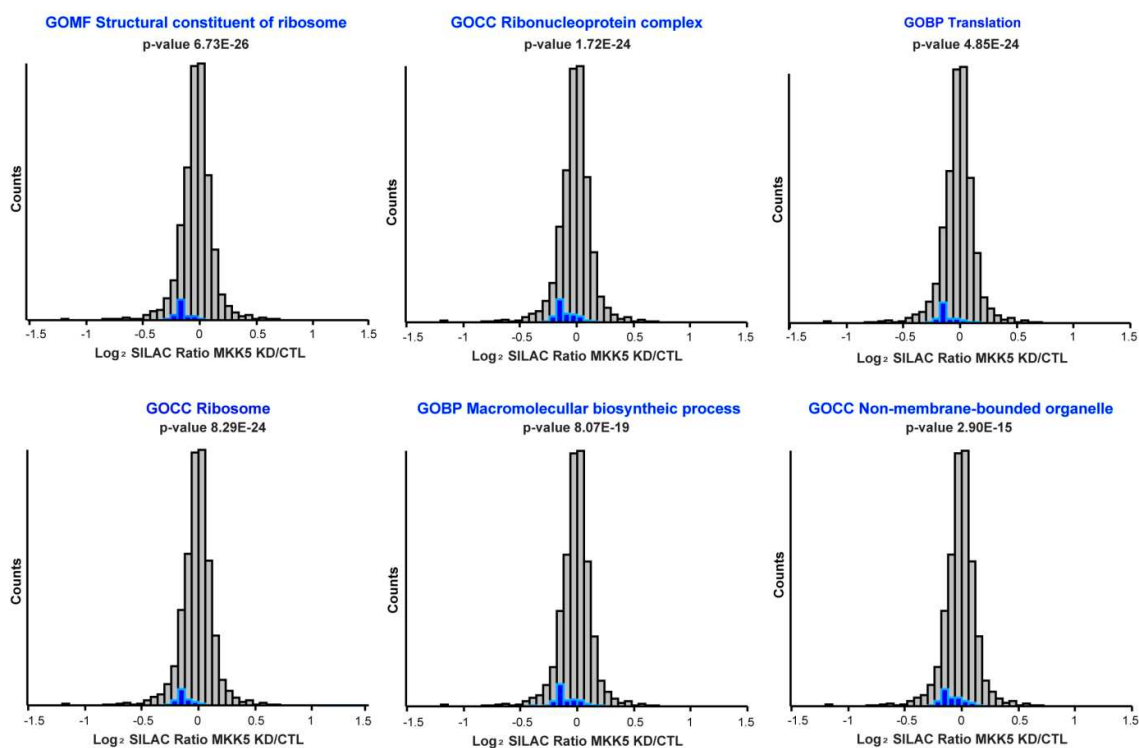


Figure 3: The unbiased 1D enrichment analysis reveals the abundance of proteins related to ribosome and translation is decreased upon MKK5 silencing. The histograms show in grey the global distribution of the quantified proteins. Highlighted in blue are the proteins belonging to the respective GO categories. The threshold used was 0.01 Benjamini-Hochberg FDR and the p-values are indicated.

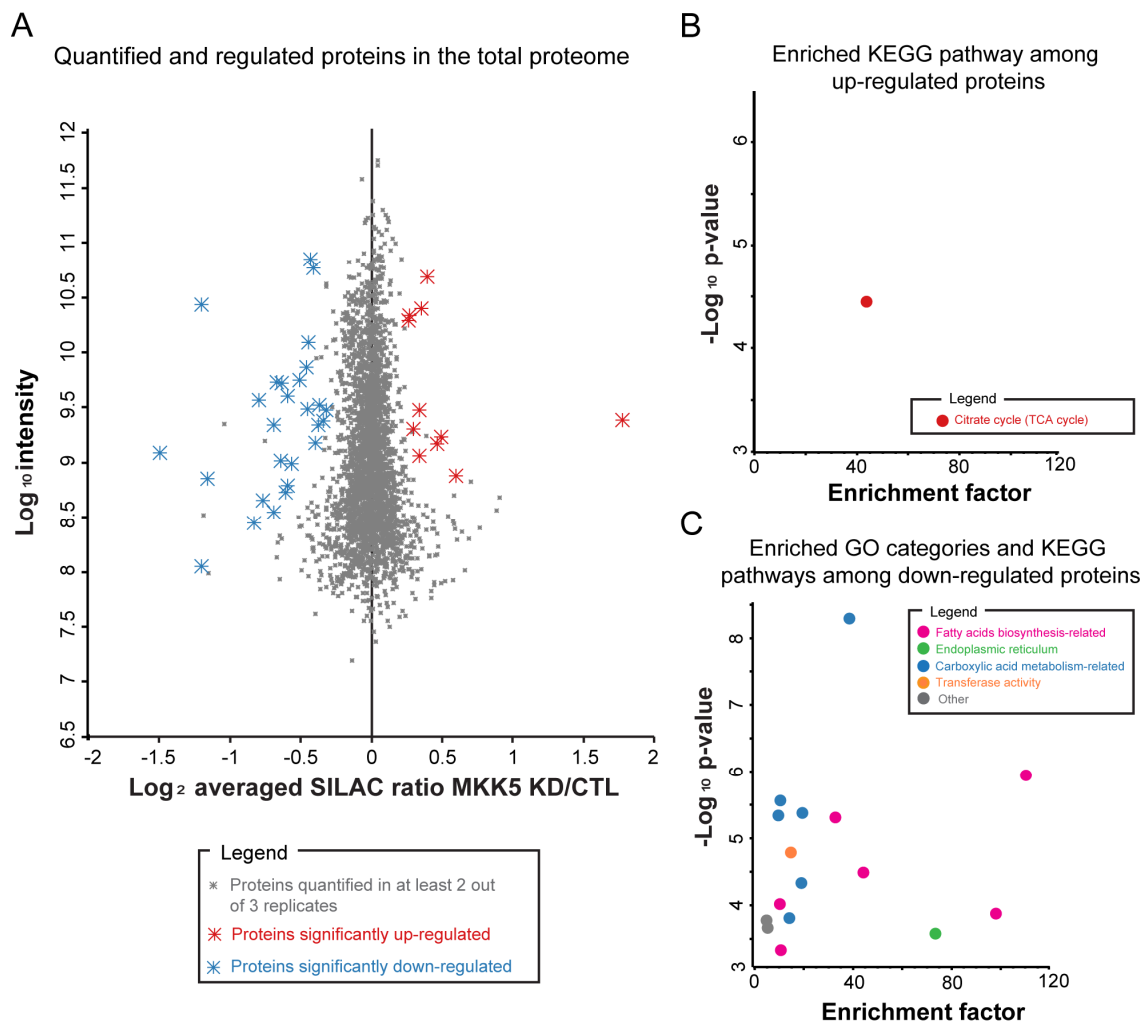


Figure 4: The silencing of MKK5 alters the total levels of proteins related to fatty acids biosynthesis and energy metabolism. (A) Scatter plot showing the quantified proteins, highlighted in red and blue are the proteins significantly regulated in at least two of three replicates determined by Significance B (0.05 Benjamini-Hochberg FDR) and with low variability across replicates. (B) Enrichment analysis of the GO categories and KEGG pathways in the subset of significantly up-regulated and (C) down-regulated proteins determined by Fisher's test (0.05 Benjamini-Hochberg FDR).

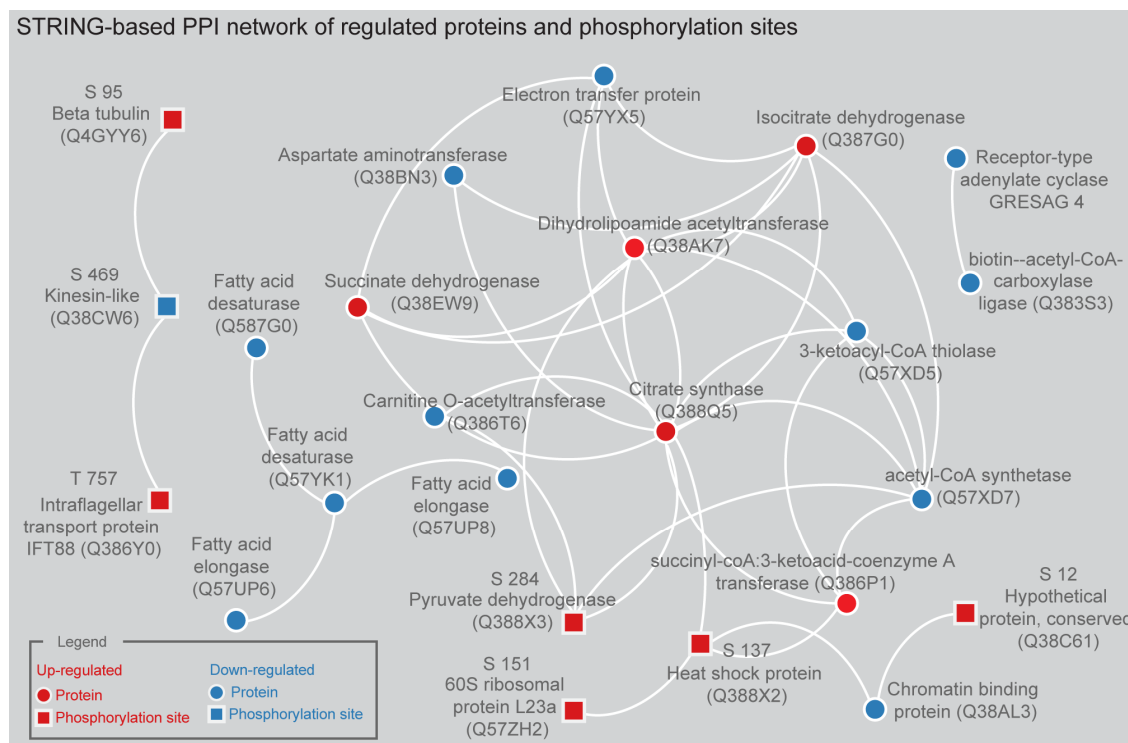


Figure 5: Functional relationship among the regulated proteins and phosphorylation sites determined by STRING. Modified residues are listed above each regulated phosphorylation sites.

Uniprot ID	Gene ID	Protein name	Log ₂ SILAC Ratio			Average	SD
			Rep 1	Rep 2	Rep 3		
Q57XQ8	Tb927.7.2160	Uncharacterized protein	1.864	1.831	1.628	1.775	0.128
Q57VC7	Tb927.5.1360	Uncharacterized protein	0.619	1.018	0.163	0.600	0.428
Q57TY7	Tb927.7.7500	Iron/ascorbate oxidoreductase family protein, putative	0.590	0.518	0.380	0.496	0.107
Q586R6	Tb927.2.4700	Uncharacterized protein	0.571	-	0.364	0.467	0.146
Q388Q5	Tb10.05.0150	Citrate synthase	0.386	0.392	0.420	0.399	0.018
Q386P1	Tb11.02.0290	Succinyl-CoA:3-ketoacid-coenzyme A transferase	0.360	0.315	0.379	0.351	0.033
Q57WY9	Tb927.3.1080	Uncharacterized protein	0.362	0.291	0.375	0.343	0.045
Q587H4	Tb927.2.2770	Uncharacterized protein	0.278	0.356	0.386	0.340	0.056
Q38EV9	Tb09.160.4480	Putative uncharacterized protein	0.239	0.337	0.309	0.295	0.050
Q38AK7	Tb10.6k15.3080	Dihydrolipoamide acetyltransferase, putative	0.263	0.303	0.246	0.271	0.030
Q387G0	Tb11.03.0230	Isocitrate dehydrogenase [NADP]	0.271	0.252	0.265	0.263	0.010
Q57Y77	Tb927.7.2670	Uncharacterized protein	-0.288	-0.294	-0.373	-0.318	0.047
Q584Q7	Tb927.6.2490	Uncharacterized protein	-0.347	-0.358	-0.314	-0.340	0.023
Q57XD7	Tb927.8.2520	Acetyl-coenzyme A synthetase	-0.364	-0.353	-0.390	-0.369	0.019
Q38BN3	Tb10.70.3710	Aspartate aminotransferase	-0.376	-0.276	-0.471	-0.374	0.098
Q57WH4	Tb927.7.3590	Uncharacterized protein	-0.326	-0.485	-0.375	-0.395	0.082
Q57XD5	Tb927.8.2540	3-ketoacyl-CoA thiolase, putative	-0.406	-0.435	-0.396	-0.412	0.020
Q57YA8	Tb927.7.2980	Uncharacterized protein	-0.386	-0.468	-0.438	-0.431	0.042
Q383S3	Tb11.01.1820	Biotin--acetyl-CoA-carboxylase ligase	-0.419	-0.439	-0.474	-0.444	0.028
Q389R7	Tb10.406.0290	Protein tyrosine phosphatase, putative	-0.502	-0.466	-0.394	-0.454	0.055
Q57UP8	Tb927.7.4180	Elongation of fatty acids protein	-0.447	-0.488	-0.445	-0.460	0.024
Q57X18	Tb927.8.5640	Uncharacterized protein	-0.463	-0.539	-0.516	-0.506	0.039
Q381P0	Tb11.01.7095	Putative uncharacterized protein	-0.535	-0.558	-0.609	-0.567	0.038
Q57YX5	Tb927.8.3380	Electron transfer protein, putative	-0.570	-0.598	-0.610	-0.593	0.020
Q587G0	Tb927.2.3080	Fatty acid desaturase, putative	-0.486	-0.712	-0.582	-0.593	0.113
Q57UP6	Tb927.7.4160	Elongation of fatty acids protein	-0.594	-	-0.620	-0.607	0.019
Q38FB9	Tb09.160.2780	Fatty acyl CoA synthetase 2	-0.609	-0.622	-0.673	-0.634	0.034
Q57VY1	Tb927.5.320	Receptor-type adenylate cyclase GRESAG 4	-0.847	-0.487	-0.586	-0.640	0.186
Q38EW9	Tb09.160.4380	Succinate dehydrogenase, putative	-0.641	-0.737	-0.630	-0.670	0.059
Q57ZJ0	Tb927.7.4990	Uncharacterized protein	-0.944	0.088	-1.207	-0.688	0.685
Q386T6	Tb11.18.0006	Carnitine O-acetyltransferase, putative	-0.699	-0.663	-0.702	-0.688	0.022
Q580N2	Tb927.3.4100	Uncharacterized protein	-0.854	-0.799	-0.648	-0.767	0.107
Q38A66	Tb10.6k15.1350	Pteridine transporter, putative	-0.719	-0.911	-0.753	-0.795	0.102
Q38AL3	Tb10.6k15.3150	Chromatin binding protein, putative	-	-1.024	-0.636	-0.830	0.274
D6XIG3	Tb927.6.4340	U6 snRNA-associated Sm-like protein	-0.426	-1.714	-1.347	-1.162	0.664
Q385F9	Tb11.02.3920	TatD related deoxyribonuclease, putative	-	-1.345	-1.051	-1.198	0.208
Q57VW9	Tb927.5.440	Trans sialidase, putative	-1.152	-1.285	-1.167	-1.201	0.073
Q57YK1	Tb927.8.6000	Fatty acid desaturase, putative	-1.400	-1.648	-1.429	-1.493	0.136

Table 1: Significantly regulated proteins upon MKK5 silencing in the total proteome.

Uniprot ID	Gene ID	Protein name	Site	Log ₂ SILAC Ratio			Average	SD
				Rep 1	Rep 2	Rep 3		
Q388X3	Tb10.389.0890	Pyruvate dehydrogenase E1 component alpha subunit, putative	S 284	1.347	1.467	1.351	1.388	0.068
Q387B6	Tb11.47.0013	Putative uncharacterized protein	S 482	1.090	1.190	1.272	1.184	0.091
Q584N4	Tb927.2.240	Retrotransposon hot spot (RHS) protein, putative	S 275	1.185	1.044	-	1.114	0.100
Q4GYY6	Tb927.1.2330	Beta tubulin	S 95	0.631	1.449	-	1.040	0.579
Q384X8	Tb11.02.4760	Putative uncharacterized protein	S 340	0.751	1.325	-	1.038	0.406
Q385G4	Tb11.02.3860	Putative uncharacterized protein	S 410	1.068	0.906	0.957	0.977	0.083
Q38C61	Tb10.70.6035	Putative uncharacterized protein	S 12	1.310	1.128	0.467	0.968	0.443
Q385Z7	Tb11.02.1680	Lectin, putative	S 454	0.882	0.925	1.002	0.936	0.061
Q57UL0	Tb927.8.5380	Ubiquitin-fold modifier 1	S 2	0.841	0.887	0.801	0.843	0.043
Q386Y0	Tb11.55.0006	Intraflagellar transport protein IFT88, putative	T 757	0.962	0.744	0.810	0.839	0.112
Q38F06	Tb09.160.3990	Cation transporter, putative	S 2	0.473	0.897	1.037	0.802	0.294
Q385B5	Tb11.02.4390	Putative uncharacterized protein	S 434	0.777	0.782	-	0.780	0.003
Q38F06	Tb09.160.3990	Cation transporter, putative	S 4	0.993	-	0.466	0.730	0.373
Q389D9	Tb10.389.1760	Putative uncharacterized protein	S 162	-	0.840	0.596	0.718	0.173
Q57XV0	Tb927.3.1170	Uncharacterized protein	S 248	0.536	0.984	0.613	0.711	0.240
Q388X2	Tb10.389.0880	Heat shock protein, putative	S 137	0.508	0.702	0.666	0.625	0.103
Q385P1	Tb11.02.2940	Ubiquitin carboxyl-terminal hydrolase, putative	S 9	0.805	0.498	0.462	0.588	0.188
Q583R5	Tb927.6.2690	Ubiquitin carboxyl-terminal hydrolase, putative	S 184	-	0.656	0.465	0.560	0.135
Q57ZH2	Tb927.7.5170	60S ribosomal protein L23a	S 151	0.697	0.586	0.293	0.526	0.209
Q57WH1	Tb927.7.3560	Uncharacterized protein	S 960	0.559	0.471	0.488	0.506	0.047
Q57YN8	Tb927.8.6370	Uncharacterized protein	S 311	-	0.528	0.479	0.503	0.035
Q57YN8	Tb927.8.6370	Uncharacterized protein	S 314	-	0.528	0.479	0.503	0.035
Q38EP6	Tb09.160.5060	Putative uncharacterized protein	T 4	0.146	0.665	0.616	0.476	0.287
Q389U9	Tb10.406.0650	Microtubule-associated protein, putative	S 2053	0.042	0.648	0.513	0.401	0.318
Q586S2	Tb927.2.4780	Uncharacterized protein	S 350	0.139	-0.611	-0.656	-0.376	0.447
Q57WH0	Tb927.7.3550	Uncharacterized protein	S 753	-0.176	-0.582	-0.595	-0.451	0.238
Q57ZR3	Tb927.5.1940	Uncharacterized protein	S 146	-0.697	-0.549	-1.130	-0.792	0.302
Q57ZR3	Tb927.5.1940	Uncharacterized protein	T 152	-0.697	-0.549	-1.130	-0.792	0.302
Q57ZR3	Tb927.5.1940	Uncharacterized protein	S 146	-0.756	-0.617	-1.057	-0.810	0.225
Q386F1	Tb11.02.1100	Nucleobase/nucleoside transporter 8.1	S 240	-	-1.552	-1.225	-1.388	0.231
Q38CW6	Tb09.244.2560	Kinesin-like protein	S 469	-2.078	-	-1.127	-1.603	0.672
Q4FKA6	Tb11.1400	Translation initiation factor eIF2B delta subunit, putative	S 207	-2.470	-2.403	-1.361	-2.078	0.622

Table 2: Significantly regulated phosphorylation sites in procyclic forms of *T. brucei* silenced for MKK5.

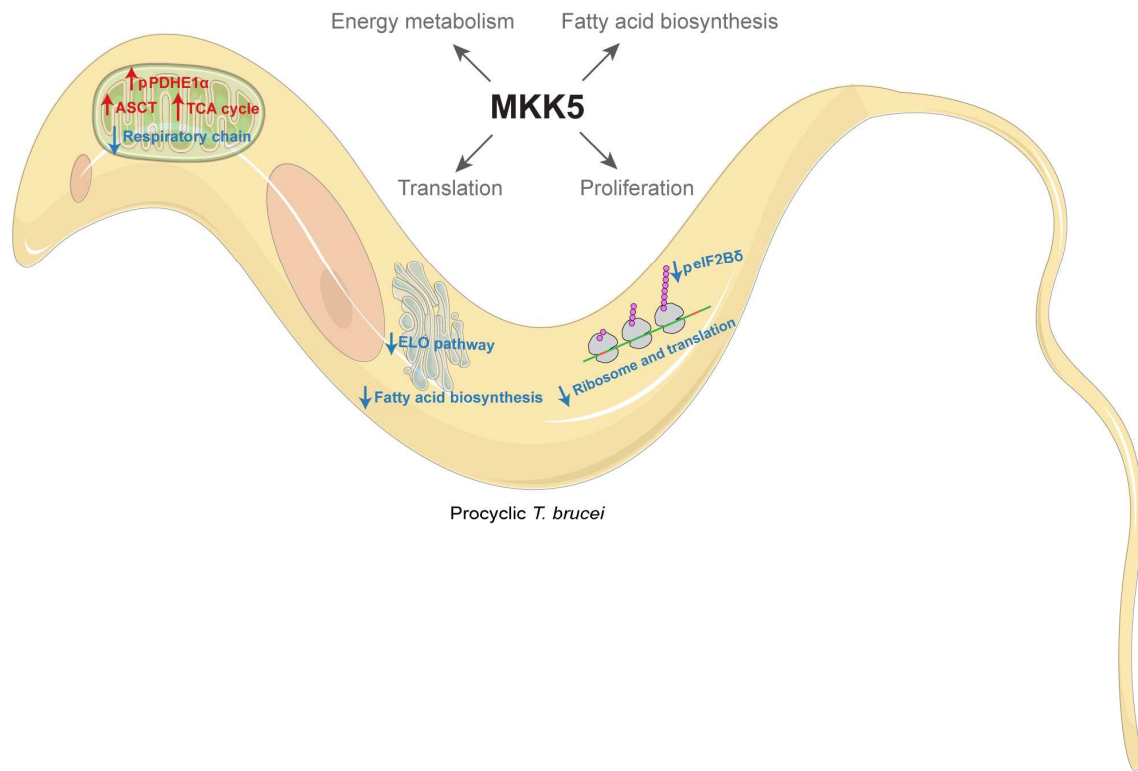
References

- 1 Matthews, K. R. The developmental cell biology of *Trypanosoma brucei*. *Journal of cell science* **118**, 283-290, doi:10.1242/jcs.01649 (2005).
- 2 Marchini, F. K., de Godoy, L. M., Batista, M., Kugeratski, F. G. & Krieger, M. A. Towards the phosphoproteome of trypanosomatids. *Sub-cellular biochemistry* **74**, 351-378, doi:10.1007/978-94-007-7305-9_15 (2014).
- 3 Parsons, M., Worthey, E. A., Ward, P. N. & Mottram, J. C. Comparative analysis of the kinomes of three pathogenic trypanosomatids: *Leishmania major*, *Trypanosoma brucei* and *Trypanosoma cruzi*. *BMC genomics* **6**, 127, doi:10.1186/1471-2164-6-127 (2005).
- 4 Qi, M. & Elion, E. A. MAP kinase pathways. *Journal of cell science* **118**, 3569-3572, doi:10.1242/jcs.02470 (2005).
- 5 Songyang, Z. *et al.* A structural basis for substrate specificities of protein Ser/Thr kinases: primary sequence preference of casein kinases I and II, NIMA, phosphorylase kinase, calmodulin-dependent kinase II, CDK5, and Erk1. *Molecular and cellular biology* **16**, 6486-6493 (1996).
- 6 Hua, S. B. & Wang, C. C. Interferon-gamma activation of a mitogen-activated protein kinase, KFR1, in the bloodstream form of *Trypanosoma brucei*. *The Journal of biological chemistry* **272**, 10797-10803 (1997).
- 7 Muller, I. B., Domenicali-Pfister, D., Roditi, I. & Vassella, E. Stage-specific requirement of a mitogen-activated protein kinase by *Trypanosoma brucei*. *Molecular biology of the cell* **13**, 3787-3799, doi:10.1091/mbc.E02-02-0093 (2002).
- 8 Ellis, J., Sarkar, M., Hendriks, E. & Matthews, K. A novel ERK-like, CRK-like protein kinase that modulates growth in *Trypanosoma brucei* via an autoregulatory C-terminal extension. *Molecular microbiology* **53**, 1487-1499, doi:10.1111/j.1365-2958.2004.04218.x (2004).
- 9 Domenicali Pfister, D. *et al.* A Mitogen-activated protein kinase controls differentiation of bloodstream forms of *Trypanosoma brucei*. *Eukaryotic cell* **5**, 1126-1135, doi:10.1128/EC.00094-06 (2006).
- 10 Guttinger, A., Schwab, C., Morand, S., Roditi, I. & Vassella, E. A mitogen-activated protein kinase of *Trypanosoma brucei* confers resistance to temperature stress. *Molecular and biochemical parasitology* **153**, 203-206, doi:10.1016/j.molbiopara.2007.02.001 (2007).
- 11 Mackey, Z. B., Koupparis, K., Nishino, M. & McKerrow, J. H. High-throughput analysis of an RNAi library identifies novel kinase targets in *Trypanosoma brucei*. *Chemical biology & drug design* **78**, 454-463, doi:10.1111/j.1747-0285.2011.01156.x (2011).
- 12 Batista, M. *et al.* The MAP kinase MAPK1 is essential to *Trypanosoma brucei* proliferation and regulates proteins involved in mRNA metabolism. *Journal of proteomics* **154**, 118-127, doi:10.1016/j.jprot.2016.12.011 (2017).
- 13 Jensen, B. C., Kifer, C. T. & Parsons, M. *Trypanosoma brucei*: Two mitogen activated protein kinase kinases are dispensable for growth and virulence of the bloodstream form. *Experimental parasitology* **128**, 250-255, doi:10.1016/j.exppara.2011.03.001 (2011).
- 14 Pan, C., Olsen, J. V., Daub, H. & Mann, M. Global effects of kinase inhibitors on signaling networks revealed by quantitative phosphoproteomics. *Molecular & cellular proteomics : MCP* **8**, 2796-2808, doi:10.1074/mcp.M900285-MCP200 (2009).

- 1
2
3
4
5
6
7
8
9
10
11
12
13
14
15
16
17
18
19
20
21
22
23
24
25
26
27
28
29
30
31
32
33
34
35
36
37
38
39
40
41
42
43
44
45
46
47
48
49
50
51
52
53
54
55
56
57
58
59
60
- 15 Hilger, M., Bonaldi, T., Gnad, F. & Mann, M. Systems-wide analysis of a phosphatase knock-down by quantitative proteomics and phosphoproteomics. *Molecular & cellular proteomics : MCP* **8**, 1908-1920, doi:10.1074/mcp.M800559-MCP200 (2009).
- 16 Bodenmiller, B. *et al.* Phosphoproteomic analysis reveals interconnected system-wide responses to perturbations of kinases and phosphatases in yeast. *Science signaling* **3**, rs4, doi:10.1126/scisignal.2001182 (2010).
- 17 Redmond, S., Vadivelu, J. & Field, M. C. RNAi: an automated web-based tool for the selection of RNAi targets in *Trypanosoma brucei*. *Molecular and biochemical parasitology* **128**, 115-118 (2003).
- 18 Wickstead, B., Ersfeld, K. & Gull, K. Targeting of a tetracycline-inducible expression system to the transcriptionally silent minichromosomes of *Trypanosoma brucei*. *Molecular and biochemical parasitology* **125**, 211-216 (2002).
- 19 Wirtz, E., Leal, S., Ochatt, C. & Cross, G. A. A tightly regulated inducible expression system for conditional gene knock-outs and dominant-negative genetics in *Trypanosoma brucei*. *Molecular and biochemical parasitology* **99**, 89-101 (1999).
- 20 Brun, R. & Schonenberg. Cultivation and in vitro cloning or procyclic culture forms of *Trypanosoma brucei* in a semi-defined medium. Short communication. *Acta tropica* **36**, 289-292 (1979).
- 21 Brenndorfer, M. & Boshart, M. Selection of reference genes for mRNA quantification in *Trypanosoma brucei*. *Molecular and biochemical parasitology* **172**, 52-55, doi:10.1016/j.molbiopara.2010.03.007 (2010).
- 22 Ong, S. E. *et al.* Stable isotope labeling by amino acids in cell culture, SILAC, as a simple and accurate approach to expression proteomics. *Molecular & cellular proteomics : MCP* **1**, 376-386 (2002).
- 23 de Godoy, L. M. *et al.* Comprehensive mass-spectrometry-based proteome quantification of haploid versus diploid yeast. *Nature* **455**, 1251-1254, doi:10.1038/nature07341 (2008).
- 24 Urbaniak, M. D., Martin, D. M. & Ferguson, M. A. Global quantitative SILAC phosphoproteomics reveals differential phosphorylation is widespread between the procyclic and bloodstream form lifecycle stages of *Trypanosoma brucei*. *Journal of proteome research* **12**, 2233-2244, doi:10.1021/pr400086y (2013).
- 25 Rappsilber, J., Ishihama, Y. & Mann, M. Stop and go extraction tips for matrix-assisted laser desorption/ionization, nanoelectrospray, and LC/MS sample pretreatment in proteomics. *Analytical chemistry* **75**, 663-670 (2003).
- 26 Rappsilber, J., Mann, M. & Ishihama, Y. Protocol for micro-purification, enrichment, pre-fractionation and storage of peptides for proteomics using StageTips. *Nature protocols* **2**, 1896-1906, doi:10.1038/nprot.2007.261 (2007).
- 27 Cox, J. & Mann, M. MaxQuant enables high peptide identification rates, individualized p.p.b.-range mass accuracies and proteome-wide protein quantification. *Nature biotechnology* **26**, 1367-1372, doi:10.1038/nbt.1511 (2008).
- 28 Cox, J. *et al.* Andromeda: a peptide search engine integrated into the MaxQuant environment. *Journal of proteome research* **10**, 1794-1805, doi:10.1021/pr101065j (2011).
- 29 Tyanova, S. *et al.* The Perseus computational platform for comprehensive analysis of (prote)omics data. *Nature methods* **13**, 731-740, doi:10.1038/nmeth.3901 (2016).
- 30 Szklarczyk, D. *et al.* STRING v10: protein-protein interaction networks, integrated over the tree of life. *Nucleic acids research* **43**, D447-452, doi:10.1093/nar/gku1003 (2015).

- 1
2
3 31 Cox, J. & Mann, M. 1D and 2D annotation enrichment: a statistical method
4 integrating quantitative proteomics with complementary high-throughput data. *BMC*
5 *bioinformatics* **13 Suppl 16**, S12, doi:10.1186/1471-2105-13-S16-S12 (2012).
- 6 32 Kimball, S. R., Fabian, J. R., Pavitt, G. D., Hinnebusch, A. G. & Jefferson, L. S.
7 Regulation of guanine nucleotide exchange through phosphorylation of eukaryotic
8 initiation factor eIF2alpha. Role of the alpha- and delta-subunits of eIF2b. *The*
9 *Journal of biological chemistry* **273**, 12841-12845 (1998).
- 10 33 Jennings, M. D. & Pavitt, G. D. A new function and complexity for protein translation
11 initiation factor eIF2B. *Cell cycle* **13**, 2660-2665, doi:10.4161/15384101.2014.948797
12 (2014).
- 13 34 Lee, S. H., Stephens, J. L. & Englund, P. T. A fatty-acid synthesis mechanism
14 specialized for parasitism. *Nature reviews. Microbiology* **5**, 287-297,
15 doi:10.1038/nrmicro1617 (2007).
- 16 35 Lee, S. H., Stephens, J. L., Paul, K. S. & Englund, P. T. Fatty acid synthesis by
17 elongases in trypanosomes. *Cell* **126**, 691-699, doi:10.1016/j.cell.2006.06.045 (2006).
- 18 36 Bringaud, F., Riviere, L. & Coustou, V. Energy metabolism of trypanosomatids:
19 adaptation to available carbon sources. *Molecular and biochemical parasitology* **149**,
20 1-9, doi:10.1016/j.molbiopara.2006.03.017 (2006).
- 21 37 Bochud-Allemann, N. & Schneider, A. Mitochondrial substrate level phosphorylation
22 is essential for growth of procyclic *Trypanosoma brucei*. *The Journal of biological*
23 *chemistry* **277**, 32849-32854, doi:10.1074/jbc.M205776200 (2002).
- 24 38 Besteiro, S., Barrett, M. P., Riviere, L. & Bringaud, F. Energy generation in insect
25 stages of *Trypanosoma brucei*: metabolism in flux. *Trends in parasitology* **21**, 185-
26 191, doi:10.1016/j.pt.2005.02.008 (2005).
- 27 39 van Hellemond, J. J., Opperdoes, F. R. & Tielens, A. G. The extraordinary
28 mitochondrion and unusual citric acid cycle in *Trypanosoma brucei*. *Biochemical*
29 *Society transactions* **33**, 967-971, doi:10.1042/BST20050967 (2005).
- 30 40 van Weelden, S. W., van Hellemond, J. J., Opperdoes, F. R. & Tielens, A. G. New
31 functions for parts of the Krebs cycle in procyclic *Trypanosoma brucei*, a cycle not
32 operating as a cycle. *The Journal of biological chemistry* **280**, 12451-12460,
33 doi:10.1074/jbc.M412447200 (2005).
- 34 41 Van Hellemond, J. J., Opperdoes, F. R. & Tielens, A. G. Trypanosomatidae produce
35 acetate via a mitochondrial acetate:succinate CoA transferase. *Proceedings of the*
36 *National Academy of Sciences of the United States of America* **95**, 3036-3041 (1998).
- 37 42 Korotchkina, L. G. & Patel, M. S. Mutagenesis studies of the phosphorylation sites of
38 recombinant human pyruvate dehydrogenase. Site-specific regulation. *The Journal of*
39 *biological chemistry* **270**, 14297-14304 (1995).
- 40 43 Patel, M. S. & Korotchkina, L. G. Regulation of the pyruvate dehydrogenase
41 complex. *Biochemical Society transactions* **34**, 217-222, doi:10.1042/BST20060217
42 (2006).
- 43 44 Nett, I. R. *et al.* The phosphoproteome of bloodstream form *Trypanosoma brucei*,
44 causative agent of African sleeping sickness. *Molecular & cellular proteomics : MCP*
45 **8**, 1527-1538, doi:10.1074/mcp.M800556-MCP200 (2009).
- 46 45 John von Freyend, S. *et al.* LmxMPK4, an essential mitogen-activated protein kinase
47 of *Leishmania mexicana* is phosphorylated and activated by the STE7-like protein
48 kinase LmxMKK5. *International journal for parasitology* **40**, 969-978,
49 doi:10.1016/j.ijpara.2010.02.004 (2010).
- 50 46 Erdmann, M., Scholz, A., Melzer, I. M., Schmetz, C. & Wiese, M. Interacting protein
51 kinases involved in the regulation of flagellar length. *Molecular biology of the cell* **17**,
52 2035-2045, doi:10.1091/mbc.E05-10-0976 (2006).
- 53
54
55
56
57
58
59
60

For TOC only



1
2
3
4
5
6
7
8
9
10
11
12
13
14
15
16
17
18
19
20
21
22
23
24
25
26
27
28
29
30
31
32
33
34
35
36
37
38
39
40
41
42
43
44
45
46
47
48
49
50
51
52
53
54
55
56
57
58
59
60